Materials Advances

ROYAL SOCIETY OF CHEMISTRY

PAPER

View Article Online
View Journal | View Issue

Cite this: *Mater. Adv.*, 2022, 3, 5138

Composite hydrogels of bacterial cellulose and an ethylene-vinyl alcohol copolymer with tunable morphological anisotropy and mechanical properties

Shun Takawa,[a] Akihide Sugawara,[a] Taka-Aki Asoh,[a] Mahasweta Nandi*[b] and Hiroshi Uyama*[a]

Anisotropic hydrogels that show a direction-dependent structure and properties have been produced and attracted attention in bio-mimicking, tissue engineering and bio-separation. Herein, bacterial cellulose (BC)-ethylene-vinyl alcohol copolymer (EVOH) composites have been prepared by precipitating EVOH within solvent-substituted BC hydrogels *via* thermally induced phase separation. The internal structures of the composites have been studied by scanning electron microscopy which reveals that the hierarchical structure characteristic of BC is retained in the composites. Depending on the production parameters of the composites like phase separation solvent composition, copolymer composition, phase separation cooling temperature and polymer concentration, the interaction between the BC and EVOH varies and the morphology changes interestingly. A stronger interaction and slow cooling rate uniformly precipitate EVOH over the BC fibers covering it, whereas a weak interaction with fast cooling induces independent precipitation of the copolymer in the BC matrix. Viscoelasticity and compressibility measurements of the composites in the hydrogel state reveal high structural and mechanical strength which are direction dependent, confirming the retention of anisotropy characteristics of the BC structure. The elastic modulus and compression strength are found to be improved significantly upon intercalation of EVOH into the BC structure giving rise to more reinforced composites. High viscoelasticity and compression strength exhibited by the composite hydrogels indicate good mechanical stability that makes them useful as replacement materials for biological tissues.

Received 22nd February 2022,
Accepted 7th May 2022

DOI: 10.1039/d2ma00204c

rsc.li/materials-advances

Introduction

Hydrogels are widely used in the areas of tissue engineering, drug delivery and biomolecule separation by bringing their physical and chemical properties closer to those that exist in nature.[1–5] Most of the biological tissues such as cartilage, striated muscle and cornea exhibit an anisotropic hierarchical structure, and thus hydrogels that can be produced with controlled anisotropy in microstructures, mechanical strength and conductivity have received a lot of attention towards such applications in recent years.[6–11] Different studies have revealed that anisotropic porous structures play an important role in cell adhesion and differentiation in the field of tissue engineering.[12–14] The control of the anisotropic shape of pores is useful in the field of separators as it reduces pressure loss and improves the selectivity of biomaterial separation.[15] Much research has been carried out on the production of such anisotropic hydrogels as they can open up new properties in the field of materials chemistry.[16] The various methods for producing anisotropic hydrogels include incorporation of carbon nanotubes, cellulose nanocrystals and inorganic nanosheets into an isotropic gel,[17–19] use of anisotropic self-assemblies as a template,[20] freeze-casting-based techniques,[21] *etc.* In this regard, bacterial cellulose (BC) biosynthesized by static culture in the presence of *Gluconacetobacter xylinus* can be a potential candidate to introduce anisotropy in composite hydrogels. In Southeast Asia, BC is also available as *nata de coco*, a familiar low calorie dessert.[22,23] Unlike plant-derived cellulose with I_β-type crystal structures, BC can be obtained in extremely pure form free from hemicellulose or lignin and characterized by an I_α-type crystal structure.[24,25]

The BC discharged from the body of the bacteria in a culture medium containing sugar remains swollen in the form of hydrogels with more than 99% of water by weight. The BC hydrogel contains nanofibers of 50–100 nm width which are grown at the culture solution/air interface in the presence of the

[a] *Department of Applied Chemistry, Graduate School of Engineering, Osaka University, Suita, 565-0871, Japan. E-mail: uyama@chem.eng.osaka-u.ac.jp*
[b] *Integrated Science Education and Research Centre, Siksha Bhavana, Visva-Bharati, Santiniketan, 731 235, India. E-mail: mahasweta.nandi@visva-bharati.ac.in*

aerobic bacteria. Thus, the gel obtained by static culture has anisotropy with a uniform nano-sized network in the planar direction and a micron-sized hierarchical lamellar structure in the growth direction.[26] The thickness, shape and strength of the resulting hydrogel can be modulated by the culture conditions.[27] Such characteristic features of the BC gel make them unique not only with respect to plant-derived cellulose but also in comparison to other polymer gels. The BC sheet obtained after drying the BC gel exhibits high mechanical strength which originates from the three-dimensional network structure of the rigid cellulose nanofibers. Apart from being a rigid polymer with excellent solvent resistance, the BC gel can replace its medium with various solvents without shrinkage, showing good moisturizing properties, biocompatibility and biodegradability. Formation of composites with organic or inorganic substances as well as other polymers can produce materials with high toughness.[28–30] In such cases, BC is used as a reinforcing material in a polymer matrix or its network structure is used as a matrix. However, there are few studies which utilize the anisotropic structural characteristics unique to the BC gel.

A polymer monolith has a continuous interconnected three-dimensional porous structure in a single piece consisting of the skeleton of the polymer network with voids.[31] Broadly, there are two methods known for preparing polymer monoliths; the polymerization method and phase separation method. The polymerization method is a technique to obtain a monolith by carrying out polymerization of a monomer solution and a cross-linking agent in the presence of a diluent, often called the porogen.[32,33] This method, however, suffers from drawbacks like difficulty in controlling the fine structure and a complicated operational procedure. On the other hand, the phase separation technique for producing a porous polymer material simply uses the process of phase separation of a polymer solution.[34] This process could be used for the production of membranes and films, but preparation of polymer monoliths that have a three-dimensional porous structure with high mechanical stability was considered to be difficult. Meanwhile, it was found that the poly(methyl methacrylate) polymer dissolved in a mixed solvent of ethanol and water can be obtained in the form of a monolith by phase separation from the solvent.[35,36] This triggered the idea of using mixed solvents for the preparation of three dimensional monolithic structures by phase separation of the polymer solutions. Subsequently, polymer monoliths from acrylic polymers other than poly(methyl methacrylate),[31,37] poly(lactic acid),[38] polycarbonate,[39] and ethylene-vinyl alcohol (EVOH)[40] copolymers have been fabricated using this technique. Such phase separation of a polymer solution in the form of a monolith can be brought about in two ways; one is thermally-induced and the other nonsolvent-induced. In thermally-induced phase separation, a polymer solution prepared by dissolution at a high temperature is cooled, whereas in poor solvent-induced phase separation, a poor solvent which reduces the solubility is added to the polymer solution. In either case, a porous structure is obtained in a neat and facile way. Thus, the use of phase separation as a technique for producing polymer monoliths has a great advantage in industrial applications due to its simplicity.

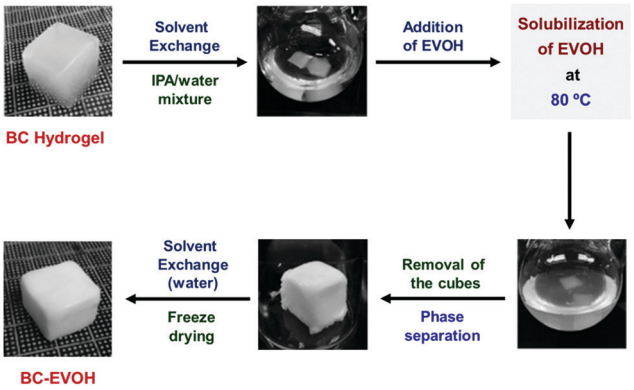

Fig. 1 Fabrication process of the BC-EVOH composite.

Based on the above advantages and characteristics and focusing on the feature that the BC gel can easily be replaced with a solvent, the current contribution reports the fabrication of composite structures by thermally induced phase separation of the EVOH copolymer from a solution inside the BC matrix (Fig. 1). The composite materials produced by this method have an anisotropic hierarchical structure derived from BC. Different conditions such as the solvent composition ratio, copolymer composition, phase separation cooling temperature and polymer concentration have been varied to ascertain their effect on the morphology, thermophysical properties, viscoelasticity and compressibility of the composites. It is found that the BC-EVOH composites show superior anisotropy in their microstructure as well as mechanical strength, making them promising candidates in the field of tissue engineering.

Experimental section

Materials and physical methods

Sodium hydroxide, hydrochloric acid and methanol were purchased from Wako Pure Chemical Industries, Ltd. Isopropyl alcohol (IPA), dimethyl sulfoxide (DMSO) and dimethylformamide (DMF) were procured from Nacalai Tesque Co. Ltd. 1-Hexanol and cellulose acetate (CA) were purchased from Sigma Aldrich. The EVOH copolymer was obtained from Kuraray Co. Ltd.[41] All the chemicals were used as purchased without any further purification. Edible *nata de coco* was purchased from Tengu Canning Co. Ltd. and was used as the source of bacterial cellulose (BC) after treatment with deionized water and sodium hydroxide.

The morphology of the composites has been studied using a SU3500 (Hitachi High Technology) Scanning Electron Microscope (SEM) operated at 15 kV. The nitrogen adsorption-desorption isotherms of the composites at liquid nitrogen temperature have been measured using a Quantachrome Nova 4200e surface area and pore size analyzer instrument. Prior to the analyses, the samples have been degassed overnight by heating at 70 °C under vacuum. The specific surface areas of the composites have been determined by the Brunauer–Emmett–Teller (BET) multipoint method and pore-size distribution by

the Non-Local Density Functional Theory (NLDFT) method. Thermogravimetric analysis (TGA) of the samples has been carried out using a SSC/7200 + TG/DTA220, Seiko Instruments. The sample weight taken was typically 3 mg and the measurement temperature was kept from 40 °C to 550 °C. The heating rate was 10 °C min^{-1} at a nitrogen gas flow rate of 150 mL min^{-1}. Differential scanning calorimetry (DSC) of the samples has been performed using EXSTAR 6000, Seiko instruments. The sample weight has been kept at 5 mg with a nitrogen gas flow rate of 50 mL min^{-1}. For the measurements, the first run was carried out from −20 to 220 °C at a heating rate of 10 °C min^{-1}, then cooling was initiated from 220 °C back to −20 °C at the same heating rate and again the second run was carried out from −20 to 220 °C keeping the heating rate unchanged.

Preparation of the composites

Purification of BC. The BC purchased commercially and preserved in syrup was impregnated in deionized water. The solvent in BC was replaced with deionized water by exchanging the deionized water about 15 times in 3 days. This BC was then added to an aqueous solution of 0.2 M sodium hydroxide and boiled. When the syrup was found to remain, discoloration and deformation were observed in BC, so its replacement with deionized water was confirmed by boiling the BC in an aqueous solution of sodium hydroxide. The BC hydrogel was finally obtained by repeated washing with deionized water until it became neutral.

Preparation of the BC-EVOH composite using IPA/water as phase separation solvent

The BC hydrogel obtained by washing with water was solvent substituted by exchanging it in a mixed solvent of IPA and water taken in a sample tube. For this purpose, the volume of water taken was equal to the volume of the BC hydrogel and the volume of IPA was adjusted so that the final volume of IPA in the mixed solvent ranged between 35 and 65%. 100 mL of IPA/water mixed solvent containing the BC gel was transferred to a 200 mL eggplant flask and EVOH was added to it keeping the concentration between 100 and 150 mg mL^{-1}. Two different EVOH copolymers, L104B and L171B, having an ethylene ratio of 27 mol% and 44 mol%, respectively, have been studied. The BC gel was refluxed with the EVOH solution in an oil bath for 3 days to fully impregnate the copolymer into the BC gel. The gel was taken out from the solution and allowed to cool to induce phase separation of EVOH in the BC gel. The phase separation cooling temperature was varied keeping it at 4 °C, 20 °C and −196 °C. Thereafter, solvent substitution was carried out with a large amount of water followed by freeze-drying to obtain BC-EVOH, a composite of BC and EVOH (Fig. 1). Simultaneously, an EVOH monolith was prepared as a reference sample. This was carried out by transferring the residual EVOH solution from which the BC/EVOH gel had been removed to a sample tube, cooling it and performing phase separation.

Apart from the BC-EVOH composite being obtained by the freeze drying method, the composite was also prepared by natural drying of the solvent. The EVOH solution impregnated BC was taken on a hot plate heated to 80 °C and allowed to stand for 2 days to dry and precipitate EVOH inside the BC. Another BC-EVOH composite was prepared using BC with clarified layers. For this, the BC hydrogel was first compressed by hot pressing for 1 minute at 80 °C and 10 MPa using a 1 mm mold. Then the compressed BC was immersed in water to swell it up slightly. After that EVOH was allowed to form a composite with the compressed BC by the above method and freeze-drying.

Viscoelasticity and compression tests

Both the measurements were performed in the hydrogel state for all the samples. The viscoelasticity tests of the samples were conducted by using a HAAKE Rheostress 6000 (Thermo Fisher Scientific), equipped with PP20 Ti, in the mode of controlled deformation (CD) at 20 °C. The measurement was performed using $\gamma = 0.005$ and keeping the measurement frequency between 0.1 and 10 Hz. Since the BC hydrogel is soft and slippery, the viscoelasticity measurement was performed by laying a filter paper moistened with water. Prior to the measurements, the BC-EVOH composite was immersed in deionized water for sufficient time and then all the six surfaces were cut with a cutter knife to obtain a hydrogel cube of *ca.* 1.5 cm × 1.5 cm × 1.5 cm. The compression tests of the samples were carried out using an EZ Graph (Shimadzu Corporation) at a compression rate of 60 mm min^{-1} and a load cell of 500 N at room temperature. The measurement was carried out in a container with deionized water to observe the drainage and re-swelling of water due to compression. In this case also, due to the slippery nature of the hydrogel, a filter paper was drawn on the container for measurement, and a hydrogel cube carved to *ca.* 1.5 cm × 1.5 cm × 1.5 cm has been used.

Results and discussion

In the preparation of the composites, the solvent within the BC gel was replaced with the EVOH solution, and then phase separation of the EVOH inside the BC gel was induced by cooling. Incorporation of the copolymer into the framework of BC can be witnessed as the translucent gel turns white due to precipitation of EVOH inside the BC gel. The phase separation behavior of EVOH inside BC can be monitored by observing the internal structure of BC-EVOH using SEM. Thus, the phase separation behavior of BC-EVOH in different composites has been investigated by changing the phase separation solvent composition ratio, copolymer composition, phase separation cooling temperature and polymer concentration. In addition to these, two other conditions have been explored; one by drying the wet composite hydrogel by natural drying of solvent and another by using a compressed BC gel for the preparation of the composite.

Internal structure control of BC-EVOH composites

Effect of the phase separation solvent composition ratio. It is known that the fabrication of EVOH monoliths can be accomplished with a wider ratio of phase separation solvent

composition than the fabrication using other polymers.[40] It is found that EVOH monoliths can be obtained keeping the IPA volume ratio between 35 and 65%. Hence, the EVOH phase separation behavior inside BC was investigated by producing BC-EVOH composites by changing the IPA volume ratio. For this study, all conditions other than the phase separation solvent composition were kept the same, with an ethylene ratio of 27 mol% in EVOH, a phase separation temperature of 4 °C and a polymer concentration of 150 mg mL^{-1}. For comparison, EVOH monoliths prepared under each condition and containing no BC were also studied. The SEM observations show that the internal structures of BC-EVOH composites differ greatly depending on the phase-separated solvent composition ratio (Fig. 2). The EVOH monolith prepared from a 65% IPA ratio shows a particle-type skeleton in which grains are continuously connected (Fig. 2a). On the other hand, in the internal structure of BC-EVOH in which phase separation has been performed in the presence of BC, no particle-type morphology can be seen (Fig. 2b). Instead, a three-dimensional network structure is observed where the fiber diameter of BC is uniformly thickened, indicating that under this condition EVOH is precipitated over the BC fibers so as to cover them evenly. Similar results can be obtained when the IPA ratio was maintained in the range of 55–45% and the EVOH copolymer got precipitated over the BC fibers forming a coating. Fig. 2d depicts the internal structure of BC-EVOH composites at 45% IPA ratio. However, when the composition ratio of IPA was set to 35%, which is the lowest amount in this variation study, it is observed that the internal structure of BC-EVOH composites is significantly different from the condition with a high IPA ratio (Fig. 2h). The BC fiber diameter does not change much due to the incorporation of EVOH. A structure different from that of BC fibers is observed with isolated lumps of the copolymer, indicating that EVOH is precipitated in the system but quite independent of BC. Under the condition of an IPA ratio of 40% (Fig. 2f), which is in between 35% and 45%, it is found that the BC fiber diameter is increased and the structure is different from that of the BC fiber. On the other hand, the effect of IPA variation on the EVOH monolith shows that with the decrease in the ratio of IPA, the particulate structure of the monolith (Fig. 2a and c) gradually disappears, and instead of that, wall-shaped structures with hollow cavities are produced (Fig. 2e and g).

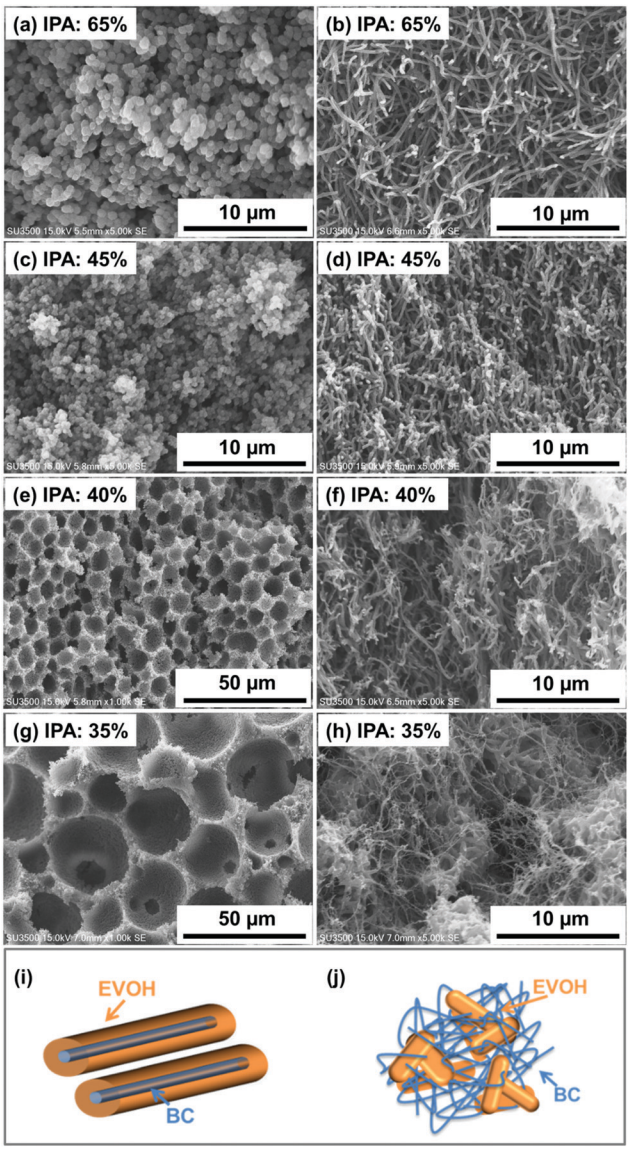

Fig. 2 SEM images of EVOH monoliths (a, c, e and g) and BC-EVOH composites (b, d, f and h) prepared at different solvent compositions and schematic representations of BC-EVOH interactions (i and j).

The factors that govern such a large change in the internal structure due to the solvent composition variation include changes in hydrogen bonding interactions between EVOH and BC as well as differences in the viscosity of the polymer solution. It is known that bacterial cellulose sheets are stabilized by strong hydrogen bonding interactions through the numerous hydroxyl groups present in their structure.[42] On the other hand, EVOH copolymers also exhibit self-association through inter and intramolecular hydrogen bonding.[41] Thus, direct observation of hydrogen bonds between BC and EVOH is difficult, since such an interaction extensively exists between the –OH groups present in the structures of BC and EVOH themselves which cannot be differentiated from the hydrogen bonds between them. However, it has been reported that BC tends to form hydrogen bonds with other polymeric structures bearing hydrogen bonding groups, including EVOH.[43,44] It is assumed that the contribution of hydrogen bonds between EVOH and BC is relatively large under the condition of a high IPA ratio. When the ratio of the more polar solvent (water) is increased, it is expected that the hydrogen bonds between BC and EVOH decrease as it interferes with the formation of such bonds. In the presence of a lower amount of water, contribution of the solvent to form hydrogen bonding between the solvent and the substrate decreases. Thus, the interaction between EVOH and BC is enhanced and precipitation of EVOH takes place uniformly over the BC fibers. This is indirect evidence of the presence of hydrogen bonds between BC and EVOH. Additionally, the internal structures of the composites change dramatically in the presence and absence of BC. In every case, the morphology of the EVOH is found to change completely

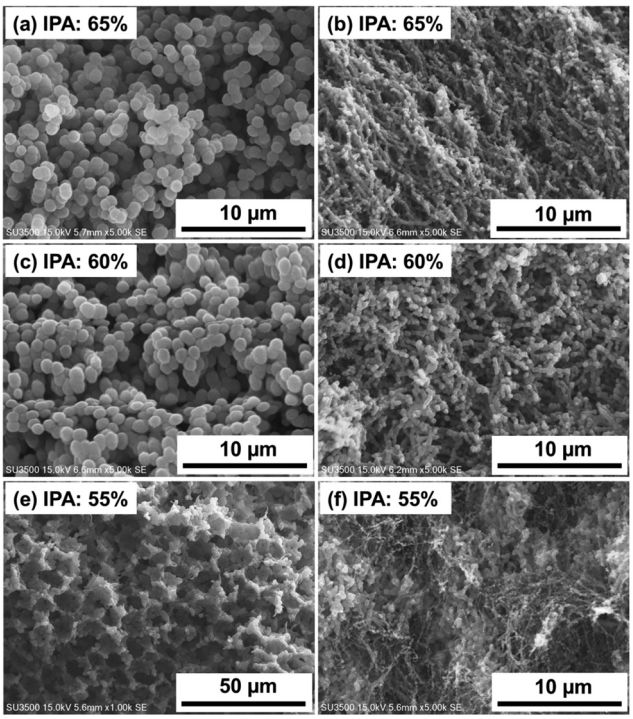

Fig. 3 SEM images of EVOH monoliths (a, c and e) and BC-EVOH (b, d and f) prepared at different solvent compositions and having ethylene content of 44 mol% in the EVOH copolymer.

on reinforcing it with BC nanofibers. This also indicates the existence of strong interactions between the EVOH copolymer and BC.

It is also observed that the viscosity of the EVOH solution increases as the IPA ratio is decreased. When phase separation is performed under the condition of high viscosity of the polymer solution, the movement of EVOH is restricted inducing rapid phase separation. This results in the precipitation of EVOH independently of the BC fibers under the condition where the IPA ratio is low. The schematic representations of the interaction of EVOH with BC are given in Fig. 2i and j. The first interaction shows how the EVOH copolymer is homogeneously deposited over the BC nanofibers forming a uniform coating when the IPA content in the mixed solvent is 65–45%. On the other hand, the second figure shows that the EVOH copolymer does not interact with the BC much and the two are precipitated quite independent of each other. Such structures are obtained when the IPA content in the mixed solvent is maintained below 40%.

Effect of the copolymer composition of EVOH

In the preceding section, it is found that the interaction between BC and EVOH has a great influence on the phase separation behavior of the composite material and hence the internal structure. In this respect, the copolymer composition is another important parameter which has been examined next in this study. BC-EVOH composites were prepared by changing the EVOH copolymer having an ethylene ratio of 27 mol% (L104B) used in previous experiments to the EVOH copolymer having an ethylene ratio of 44 mol% (L171B). In this study as well, the internal structure is observed by changing the phase separation solvent composition, and the study was conducted with 55–65% IPA which can produce EVOH (L171B) monoliths. The conditions other than the solvent composition were maintained the same and the EVOH copolymerization ratio was examined under the conditions of an ethylene ratio of 44 mol%, a phase separation temperature of 4 °C, and a polymer concentration of 150 mg mL^{-1}. The EVOH monoliths containing no BC under each condition were also studied. SEM images of BC-EVOH composites and EVOH monoliths prepared under each condition are illustrated in Fig. 3. The figures show that the internal structure of BC-EVOH changes significantly depending on the solvent composition ratio even when the ethylene ratio is 44 mol%. The cross-sections of the monoliths shown in Fig. 3a, c and e are found to exhibit particle morphology at an IPA ratio of 65 and 60%, which changes to a wall-like structure with cavities at an IPA ratio of 55%. In the case of the composites, at 65% IPA ratio, granular EVOH is observed to be precipitated covering the BC fibers (Fig. 3b). A similar internal structure is also observed under the condition of 60% IPA (Fig. 3d). However, when the IPA ratio is decreased to 55%, a different internal structure is formed (Fig. 3f). Though a small amount of granular EVOH is precipitated on the BC fiber, a substantial amount of EVOH aggregates is found to be precipitated independent of the BC fibers. In the case of EVOH with an ethylene ratio of 44 mol%, the number of hydroxyl groups is less than that with an ethylene ratio of 27 mol%. Thus, it can be anticipated that the hydrogen bonds formation by EVOH with BC is reduced in the case of the EVOH with higher ethylene content. The EVOH with a higher proportion of ethylene forms an independent three-dimensional structure even at a higher IPA ratio, as compared to the EVOH with lower ethylene content. These results indicate that the hydrogen bonding between BC and EVOH has a great influence on the internal structure of BC-EVOH composites.

Effect of phase separation cooling temperature

It is known that the skeleton diameter of EVOH monoliths changes depending on the phase separation cooling temperature.[40] Therefore, the effect of phase separation cooling temperature on the internal structure of BC-EVOH has been investigated. All conditions other than the phase separation cooling temperature were kept the same; the EVOH taken for the study has a copolymerization ratio of 27 mol% of ethylene and the polymer concentration is 150 mg mL^{-1}. EVOH monoliths containing no BC under each condition have also been examined. At first the BC-EVOH composites were prepared at a phase separation temperature of 20 and −196 °C using an IPA ratio of 65%, and it is found that EVOH is precipitated over the BC fibers to cover them uniformly, similar to that observed at 4 °C. Thus, under the condition of 65% IPA, no difference in the internal structure is observed depending on the phase separation cooling temperature. However, the structures of the EVOH monoliths and BC-EVOH composites prepared at an IPA ratio of 35% show significantly different results. Under this condition, a wall type morphology is observed for the EVOH monoliths at all

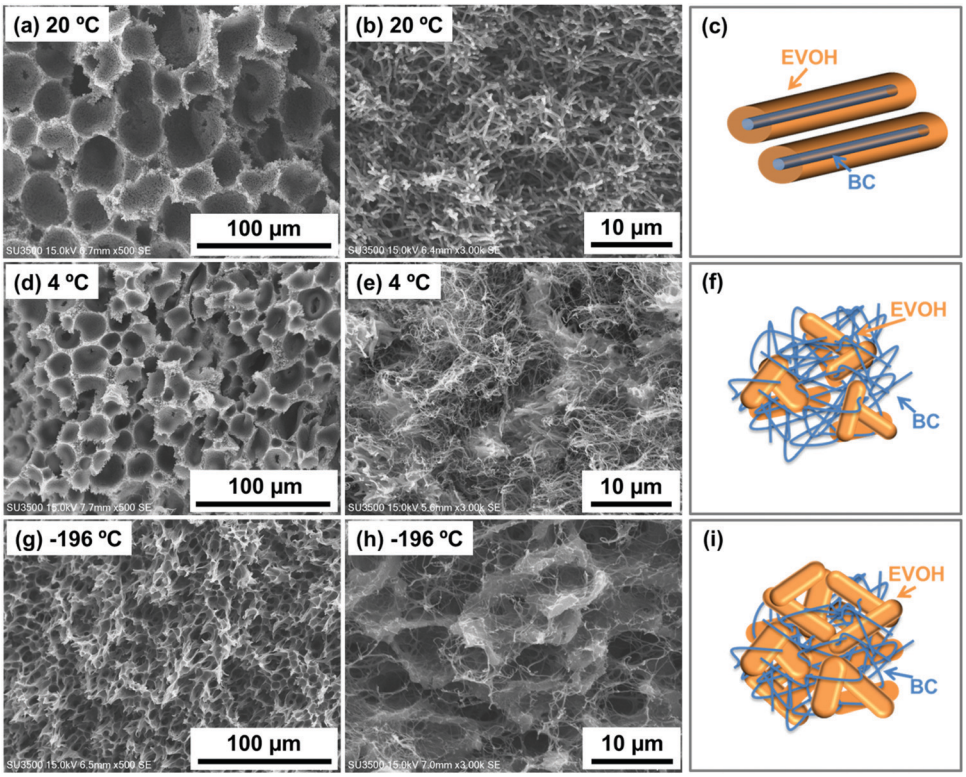

Fig. 4 SEM images of EVOH monoliths (a, d and g) and BC-EVOH (b, e and h) prepared at different cooling temperatures (solvent composition: IPA 35%) and schematic representations of BC-EVOH interactions (c, f and i).

temperatures of phase separation (Fig. 4a, d and g) but the skeleton size decreases with the decrease in temperature. Somewhat interesting results are obtained for the BC-EVOH composites prepared in 35% IPA and a clear change in the internal structure could be observed depending on the cooling temperature (Fig. 4b, e and h). As discussed earlier, at 4 °C, EVOH is found to precipitate independently without any interaction with the BC fibers (Fig. 4e). However, when the cooling temperature was set higher at 20 °C, EVOH did not precipitate independently (Fig. 4b) but covered the BC fibers forming a coating over them as observed at an IPA ratio of 45% or higher. When the BC-EVOH composites were prepared by gradually lowering the cooling temperature, it is found that between 4 and 15 °C, EVOH was precipitated independently of the BC fibers and formed aggregates within the fibers. When the cooling temperature was further lowered to −196 °C (Fig. 4h), it is observed that EVOH formed an independent three-dimensional network skeleton between the BC fibers. The schematic representations of the interaction between BC and EVOH at different temperatures have been illustrated in Fig. 4c, f and i. From these results, it can be concluded that the phase separation behavior of EVOH in BC changes drastically with temperature.

Effect of polymer concentration

It has been reported that in the fabrication process of monoliths the skeleton diameter is dependent on the polymer concentration.[31] Therefore, the effect of polymer concentration

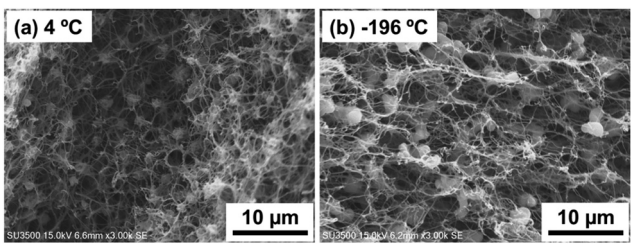

Fig. 5 SEM images of BC-EVOH composites prepared at cooling temperatures of (a) 4 °C and (b) −196 °C (polymer concentration: 100 mg mL^{-1} and solvent composition: IPA 35%).

on the internal structure of BC-EVOH composites has been examined by changing the concentration to 100 mg mL^{-1} from 150 mg mL^{-1} used in previous studies (Fig. 5). Except for the polymer concentration, all other conditions are maintained the same. The EVOH copolymer with an ethylene ratio of 27 mol% is taken and the phase separation has been studied at temperatures of 4 and −196 °C. At first, the studies are performed in 65% IPA solution and it is found that EVOH is precipitated over the BC fibers evenly just as in the case of 150 mg mL^{-1} concentration. There is no change due to the polymer concentration or the phase separation temperature and EVOH precipitates to cover the BC fibers in the same manner. On the other hand, in 35% IPA solution and at a phase separation temperature of 4 °C where EVOH is found to precipitate and aggregate between BC fibers at 150 mg mL^{-1} (Fig. 2h), different

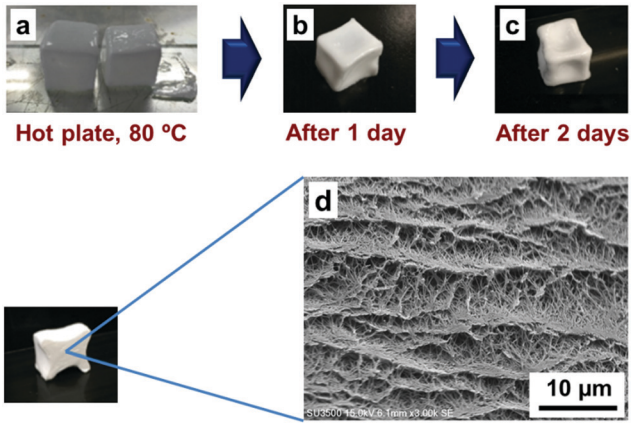

Fig. 6 (a–c) Natural drying of BC-EVOH on a hot plate and (d) SEM image of the resulting composite.

behavior is observed at a polymer concentration of 100 mg mL^{-1}. The EVOH is found to aggregate into small particles and precipitate (Fig. 5a). However, at a cooling temperature of −196 °C, EVOH forms a network-like skeleton between the BC fibers at 150 mg mL^{-1} concentration (Fig. 4h), and at a polymer concentration of 100 mg mL^{-1} particulate aggregates are deposited continuously with sufficient network-like skeleton formation (Fig. 5b). From these results, it can be concluded that polymer concentration is also an important factor towards the phase separation behavior of EVOH on BC fibers.

Effect of natural drying of solvent

In this study all other conditions were maintained the same with an EVOH copolymerization ratio of 27 mol%, a polymer concentration of 150 mg mL^{-1} and 65% IPA, except that EVOH was allowed to precipitate inside the BC by drying on a hot plate at 80 °C (Fig. 6a). After one day of drying, the surface becomes dry and hard, but the inside remains gel-like (Fig. 6b). After further drying for another two days, the inside of the composite dries up completely (Fig. 6c). The BC-EVOH composite obtained shows shrinkage on the surface, but it is found to maintain its morphology inside. When the internal structure of the dried BC-EVOH was observed by SEM, the BC layers can be clearly observed with the EVOH copolymer precipitated uniformly to cover the BC fibers (Fig. 6d). On the other hand, BC to which EVOH was not added shrunk completely due to dryness and becomes a sheet. The reason behind the BC layers being clearly visible here is that some layers come in close contact with each other when the solvent is vaporized due to natural drying in air rather than freeze-drying or vacuum drying.

Effect of using compressed BC with clarified layers

It is observed that EVOH is deposited independently instead of covering the BC fibers in 35% IPA and low phase separation temperature. Thus, by compressing the BC gel to get clarified layers, a study of the internal structure of BC-EVOH composites prepared using the compressed BC gel was carried out (Fig. 7). For this study, the copolymerization ratio of the EVOH is

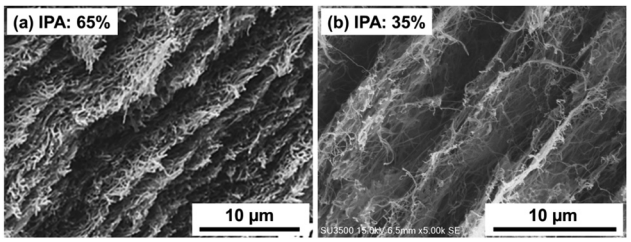

Fig. 7 SEM images of layered structures of BC-EVOH composites prepared using compressed BC at a solvent composition of (a) IPA: 65% and (b) IPA: 35%.

27 mol% of ethylene, the polymer concentration is 150 mg mL^{-1} and the phase separation temperature is 4 °C. From the SEM image, the morphology between the layers is observed with clarity by re-swelling the BC gel after hot pressing. It is observed that EVOH is precipitated so as to cover the BC fibers at 65% IPA (Fig. 7a) whereas EVOH precipitates independent of BC under the condition of 35% IPA (Fig. 7b). Apart from this, the precipitation of EVOH is observed to be concentrated in the dense layers of the BC fibers.

Determination of water content in the composites

The water contents of the composites have been determined by gravimetric analysis.[45] For this, the weights of the BC-EVOH composites were taken before and after removal of the surface water, and the water content was calculated using the following equation:

$$\text{Water content } (\%) = \frac{w_1 - w_0}{w_1} \times 100$$

where w_0 is the weight of the composites after drying by lyophilization and w_1 is the weight of the composites after removal of excess water and before drying.

The results show that the water contents of all the composites, irrespective of the IPA content and cooling temperature, remain between *ca.* 86 and 87%. Thus, the polymer content in the composites ranges between *ca.* 13 and 14.5%. The water content of the BC hydrogel itself is 99.0–99.5% and the EVOH copolymer concentration taken is 150 mg mL^{-1}. Furthermore, the size of the BC hydrogel cubes remained almost unchanged in the fabrication of the composites. Thus, it can be anticipated that the EVOH copolymer is incorporated into the BC hydrogel cubes and retained inside after phase separation.

Nitrogen adsorption–desorption studies

Nitrogen sorption studies have been carried out to understand the porosity and pore structure of the composites and the results are shown in Fig. 8. The BET surface areas of the various BC-EVOH composites are given in Table 1. The surface area of the composites prepared under the condition of 35% IPA is found to increase with the increase in cooling temperature. For cooling temperatures of −196, 4 and 20 °C the surface areas are found to be 9.6, 17.5 and 28.2 $m^2\ g^{-1}$, respectively. On the other hand, for 65% IPA and a cooling temperature of 4 °C, the surface area is 20.6 $m^2\ g^{-1}$. However, these values of surface

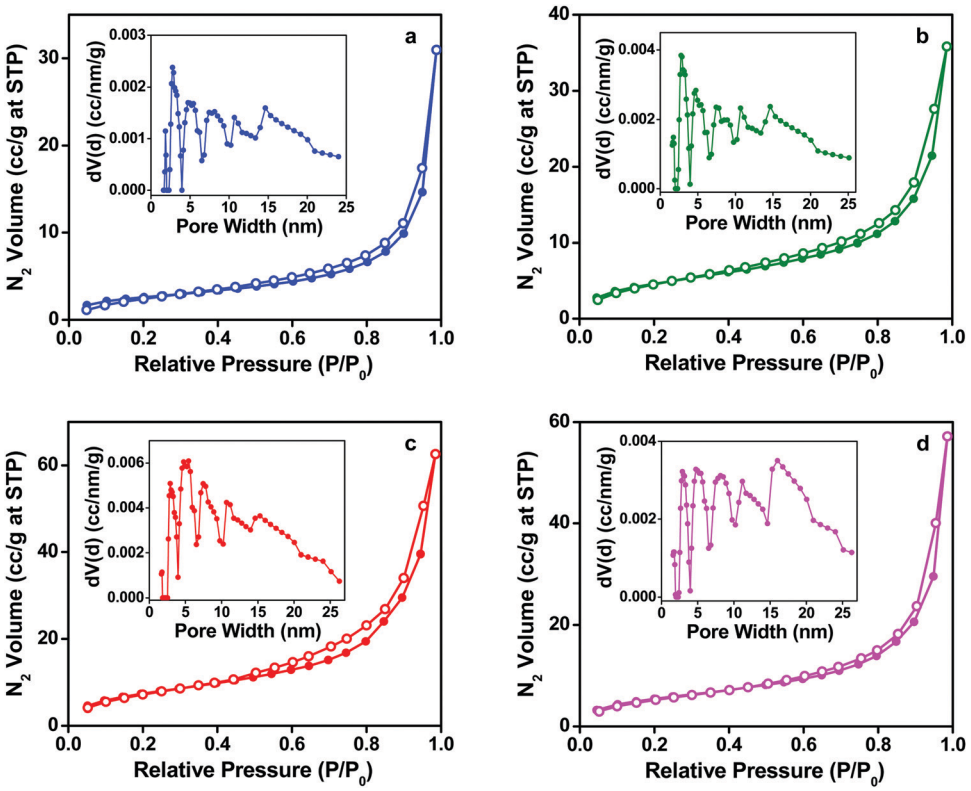

Fig. 8 Nitrogen adsorption–desorption isotherms of BC-EVOH composites prepared at different solvent compositions and cooling temperatures of (a) IPA 35% and −196 °C, (b) IPA 35% and 4 °C, (c) IPA 35% and 20 °C and (d) IPA 65% and 4 °C. Adsorption points are marked by filled symbols and desorption points are marked by empty symbols. Insets: pore size distribution of the corresponding composites obtained by using the NLDFT method.

areas are not considerably high as compared to those of samples containing mesopores. The isotherms can be classified as type-III,[46] typical of nonporous samples or samples containing very large pores with weak adsorbate–adsorbent interactions. Thus, the skeleton structures of the composites have only macropores as depicted in the electron microscopy images with the absence of formation of any mesopores. The same conclusion can be drawn from the pore size distribution plots of the samples given in the inset of the figures which shows a broad spread over a large range of pore diameters. These results suggest that the EVOH copolymer gets coated over the cellulose fiber of BC, without the formation of pores in the nanoporous region. Thus, the mass flow within the matrices of the composites can take place through the macropores having an interconnected porous structure thereby promoting the migration of nutrients and other growth factors inside the material.[45]

Table 1 Water content and surface area of BC-EVOH composites

	Mixed solvent composition	Phase separation temperature (°C)	Water content (%)	BET specific surface area ($m^2\ g^{-1}$)
BC-EVOH composite	IPA 35%	−196	85.6	9.6
		4	86.5	17.5
		20	87.1	28.2
	IPA 65%	4	86.0	20.6

Thermophysical properties

BC-EVOH composites. It has been found that composite materials often show improved thermal stability as compared to the individual components present in them.[47] Therefore, the thermophysical properties of the BC-EVOH composites have been investigated by TG and DSC measurements. The TG curves for BC-EVOH prepared under the condition of 35% IPA with phase separation temperatures of 20, 4 and −196 °C, and 65% IPA at a phase separation temperature of 4 °C have been shown in Fig. 9. The results show that only the BC-EVOH composite which has been prepared under the conditions of 35% IPA and −196 °C could improve the thermal stability of the EVOH monolith by combining with BC. However, under this condition EVOH forms an independent three-dimensional network between the BC fibers instead of being uniformly coated over BC. It can be considered that such a result will have a great influence on the crystallinity. Therefore, DSC measurements were carried out to examine the crystallinity of these BC-EVOH composites and the results are given in Fig. 10. From the results, the melting point (T_m), the enthalpy change at the melting point (ΔH_m) and the crystallinity (X_c) of the samples have been calculated and are given in Table 2. While calculating X_c, it is assumed that $\Delta H_m^{EVOH} = \alpha \Delta H_m^{PVA}$, where α is the mole fraction of the PVA (poly(vinyl alcohol)) part in EVOH. When the crystallinity of PVA is 100%, the ΔH_m^{PVA} is 156.2 J g^{-1}.[48]

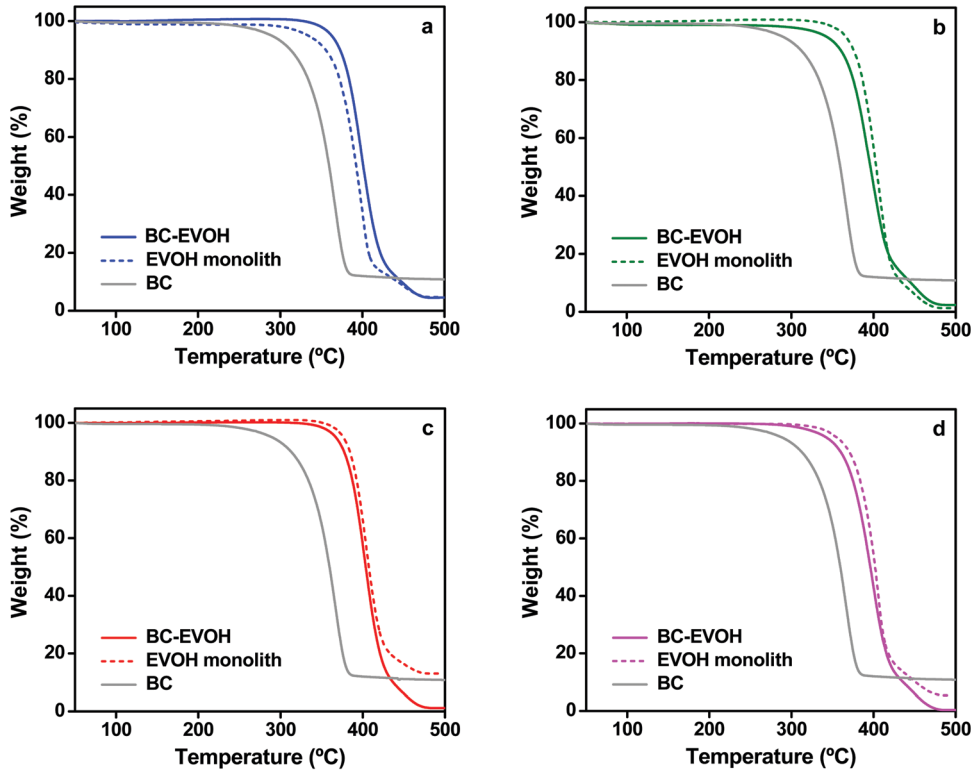

Fig. 9 Thermogravimetric analysis of BC, EVOH monoliths and BC-EVOH composites prepared at different solvent compositions and cooling temperatures of (a) IPA 35% and −196 °C, (b) IPA 35% and 4 °C, (c) IPA 35% and 20 °C and (d) IPA 65% and 4 °C.

As can be expected from the different internal structures, the crystallinity of BC-EVOH composites varies greatly depending on the preparation conditions. Even under the cooling conditions of −196 °C and 4 °C where EVOH is precipitated independently of the BC fibers different results can be observed. On the other hand, for the EVOH monolith the crystallinity of the rapidly cooled product decreases due to the increase of the amorphous part. However, in the BC-EVOH composite, the crystallinity is found to be higher under the quenching condition of −196 °C, whereas the crystallinity produced under the condition of 4 °C is very low. This may occur due to the inhibition of crystal growth of EVOH by BC fibers at 4 °C, while such an effect of BC fibers on EVOH is not observed at −196 °C due to rapid phase separation.

Anisotropy in the composites

Viscoelasticity test. The anisotropy of BC and BC-EVOH composite materials has been examined by the viscoelasticity test in their hydrogel state (Fig. 11). For the BC hydrogel alone, there is a difference in elastic modulus between the perpendicular direction and the parallel direction with respect to the layered structure of BC (Fig. 11a and b); the result shows that the value is higher in the parallel direction. Subsequently, in BC-EVOH similar anisotropy has been observed, and it is found that the elastic modulus is higher in the parallel direction (Fig. 11c). From this result, it is observed that the anisotropy derived from the BC hierarchical structure is retained in the composites even after intercalation of EVOH into the framework. Apart from this, the elastic modulus is found to improve greatly upon incorporation of EVOH into the BC structure. Thus, it can be concluded that as a result of combination of BC and EVOH, the viscoelasticity of the resulting composite increased drastically. The elastic moduli at a frequency of 1.0 Hz are summarized and the difference between the vertical and horizontal directions in each sample has been calculated (Fig. 11d). It is found that the anisotropy in the BC-EVOH composite prepared in 65% IPA, where the polymer is precipitated so as to cover the BC fiber, is larger than that prepared in 35% IPA, in which the polymer is precipitated independent of BC.

Compression test. The anisotropy of BC and BC-EVOH composite materials has also been examined by the compression test in their hydrogel state (Fig. 12). For the BC hydrogel alone, there is again a difference in compression strength between the perpendicular direction and the parallel direction with respect to the BC hierarchical structure. In this case too, the result showed that the compression strength is higher in the parallel direction (Fig. 12a and b). When the compressibility of BC-EVOH composites was measured, similar anisotropy was observed and it is found that the intensity is higher in the parallel direction (Fig. 12b). The compression in the parallel direction shows higher stress than the compression in the vertical direction throughout the entire strain range.[49] This can be attributed to the fact that the planar fiber layer of BC stacked vertically one over another has the capability to take higher stress than the layer placed horizontally. A similar observation can be found with BC hydrogel cubes as well.

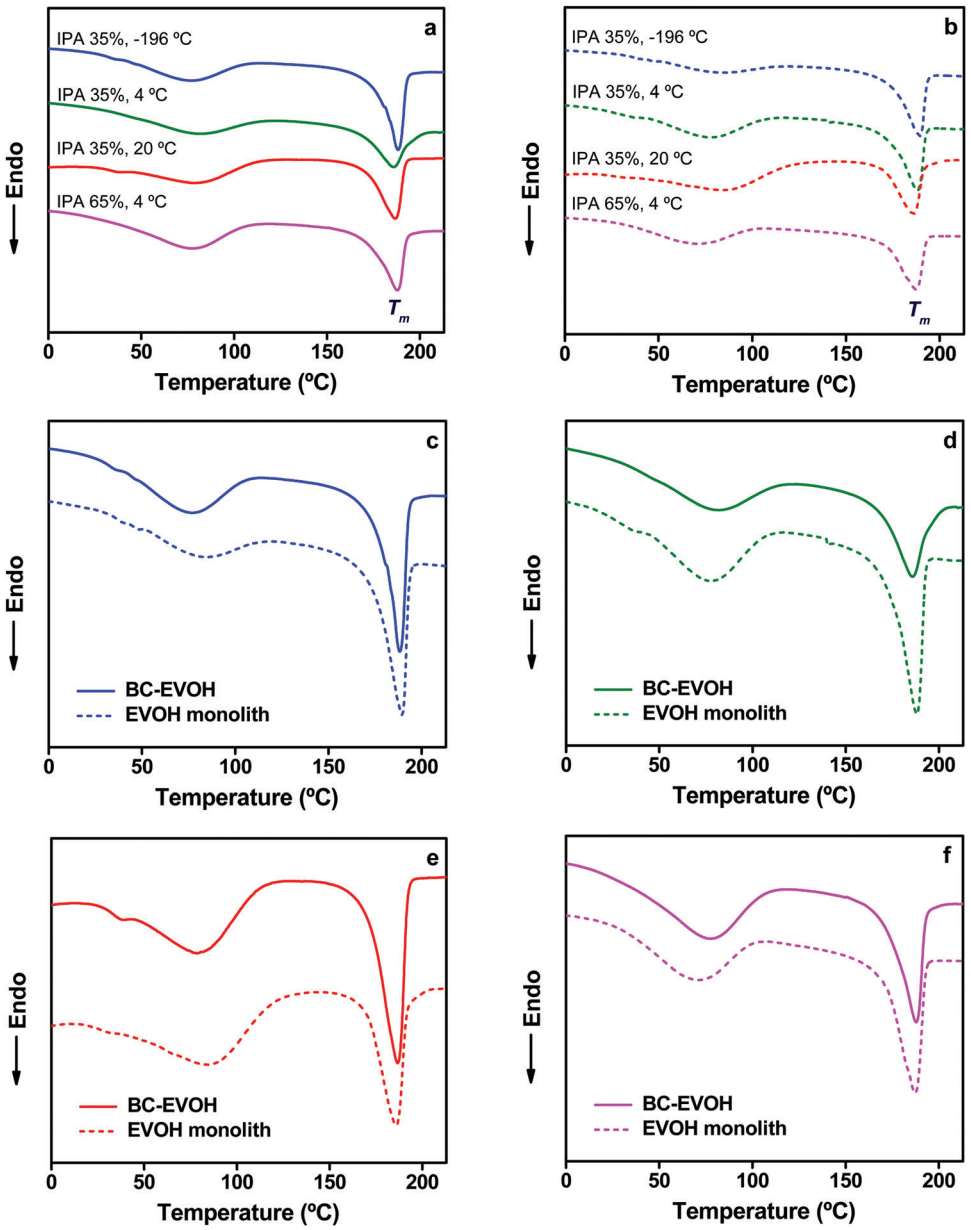

Fig. 10 DSC analyses of all (a) BC-EVOH composites and (b) EVOH monoliths. Individual DSC plots of BC-EVOH composites and EVOH monoliths prepared at different solvent compositions and cooling temperatures of (c) IPA 35% and −196 °C, (d) IPA 35% and 4 °C, (e) IPA 35% and 20 °C and (f) IPA 65% and 4 °C.

Table 2 Thermal properties of BC-EVOH composites and EVOH monoliths obtained by DSC

	Mixed solvent composition	Phase separation temperature (°C)	T_m (°C)	ΔH_m (J g^{-1})	X_c (%)
BC-EVOH composite	IPA 35%	−196	188	71.3	62.5
		4	187	61.2	53.7
		20	189	70.0	61.4
	IPA 65%	4	188	64.0	56.1
EVOH monolith	IPA 35%	−196	190	70.7	62.0
		4	188	77.1	67.6
		20	188	69.8	61.2
	IPA 65%	4	187	71.8	63.0

Thus, it is observed that the anisotropy derived from the BC hierarchical structure is retained in the compression test even after composite formation with EVOH. In this case too, it is observed that the compression strength of the composite is greatly improved due to compounding the BC fibers with the EVOH copolymer. The tangential elastic modulus has been calculated at a compressive strain of 50% (ε = 45–55%) and the difference in the values between the vertical direction and the horizontal direction in each sample is given in Fig. 12c. The results show that the BC-EVOH composite prepared in 65% IPA, in which the polymer is precipitated over the BC fiber to cover them, has increased anisotropy than the original BC hydrogel

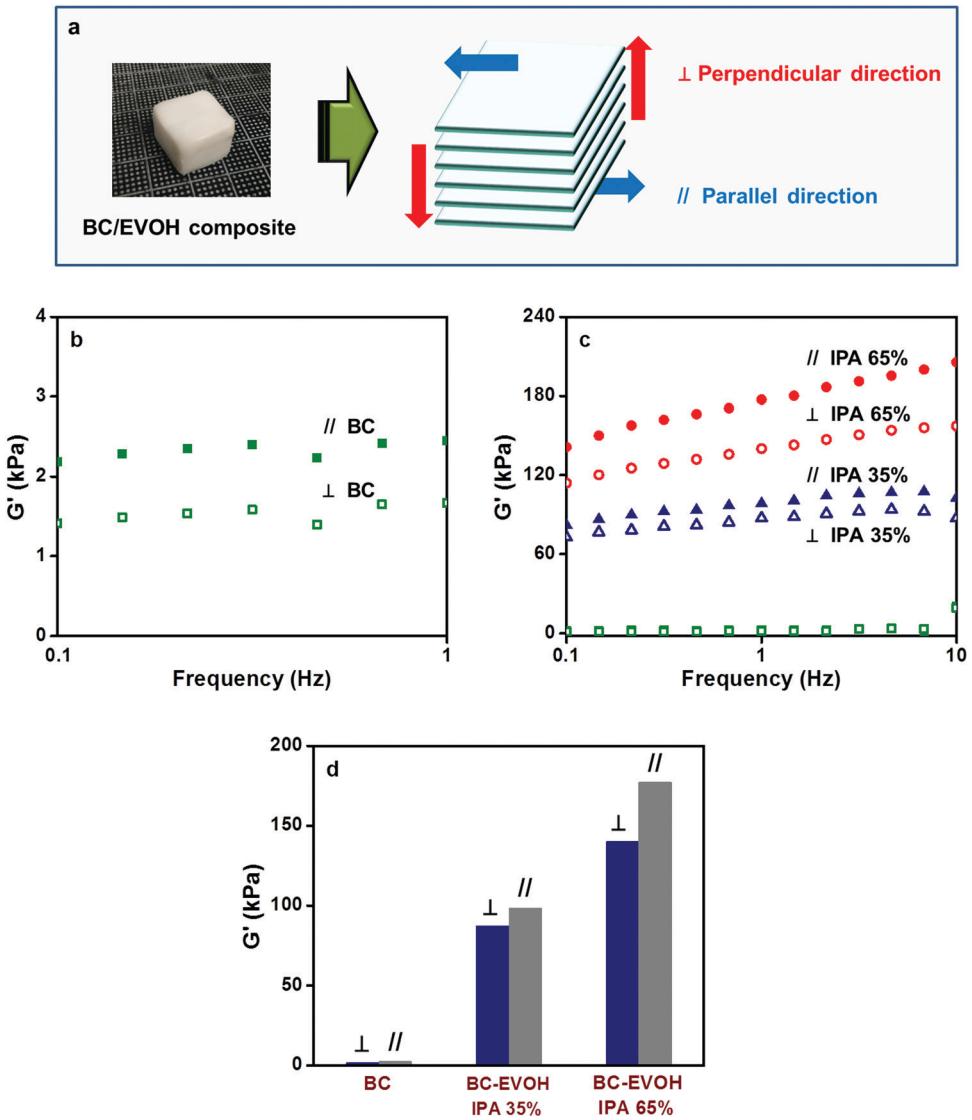

Fig. 11 (a) Schematic representation for shear deformation of the BC hydrogel and BC/polymer composite. Storage moduli of (b) BC hydrogel and (c) BC-EVOH composites prepared at 4 °C in solvent compositions of 35% and 65% IPA. The parallel direction is shown by closed symbols and the perpendicular direction by open symbols. (d) Storage moduli of BC and BC-EVOH composites at 1.0 Hz along different directions.

alone. On the other hand, in the BC-EVOH composite with an IPA ratio of 35%, where the polymer is precipitated independently of BC, anisotropy derived from BC is observed. The anisotropy is smaller than that of the composite with 65% IPA but higher than that of the original BC hydrogel alone. From the above results, it can be inferred that the anisotropy can also be controlled by controlling the internal structure of the BC-EVOH composite material under various preparation conditions.

Conclusions

BC-EVOH composites have been prepared by solvent substitution of the BC gel and thermally induced phase separation of the EVOH solution. SEM images confirm that the composite materials maintain the hierarchical structure derived from BC. The phase separation behavior of BC-EVOH is found to depend on several parameters like phase separation solvent ratio, copolymer composition, phase separation cooling temperature and polymer concentration. When the interaction between EVOH and BC fibers is strong and phase separation is induced over time at higher temperature, EVOH precipitates over the BC fibers thereby covering them uniformly. On the other hand, under the condition that the interaction between EVOH and BC fibers is relatively weak and the phase separation is induced rapidly at low temperature, EVOH is precipitated independently between the BC fibers. Thus, the internal structure can be controlled by altering the preparation conditions and accordingly the thermal stability of the composites is found to vary. In each case, the composites have been compared with the EVOH monoliths and the change in the morphological features can be

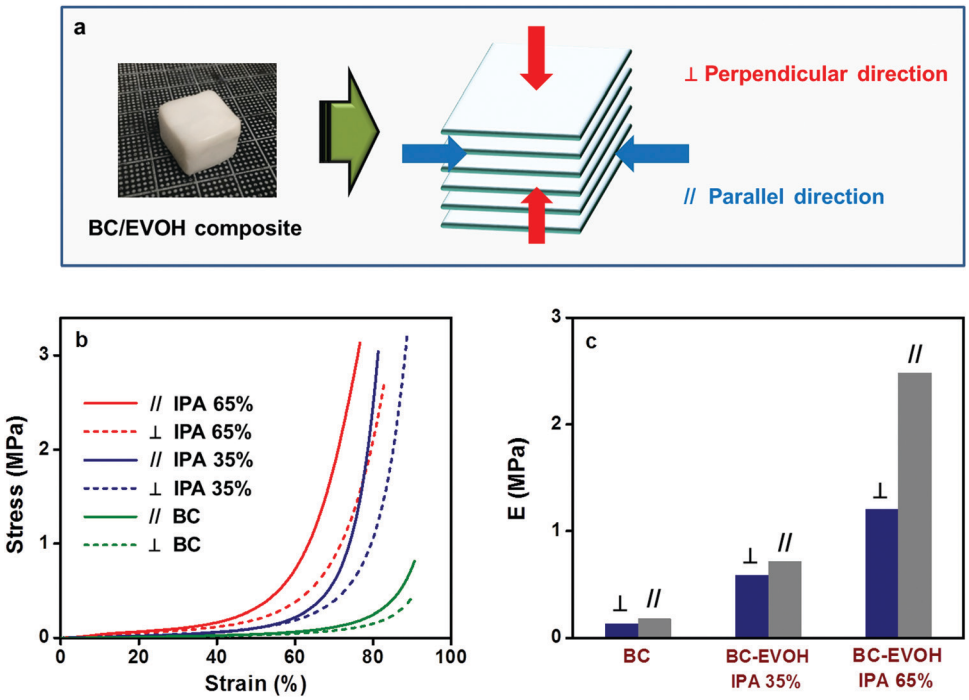

Fig. 12 (a) Schematic representation for compress deformation of the BC hydrogel and BC/polymer composite. (b) Stress strain curves of the BC hydrogel and BC-EVOH composites prepared at 4 °C at solvent compositions of 35% and 65% IPA. The parallel direction is shown by solid lines and the perpendicular direction by dashed lines. (c) Tangent elastic moduli storage moduli of BC and BC-EVOH composites at ε = 50% along different directions.

clearly witnessed. In the viscoelasticity and compression tests, anisotropy can be observed in the direction perpendicular and parallel to the growth direction of the BC layers, indicating that the porous composite materials retain the anisotropy of the BC hierarchical structure. However, the elastic modulus and compression strength have been found to improve greatly upon incorporation of EVOH into the BC structure to form the composites. The anisotropy is found to be higher in the structures where the EVOH copolymer precipitates covering the BC fibers rather than the structures where EVOH is precipitated independently. Such controllable morphology and hydrogel anisotropy provide a versatile technique for the preparation of anisotropic hydrogels characterized by biocompatibility as well as bio-mimicking properties.

Conflicts of interest

There are no conflicts to declare.

Acknowledgements

H. U. thankfully acknowledges financial support from the JST-Mirai Program (JPMJMI18E3) and JSPS KAKENHI Grants (20H02797). M. N. gratefully acknowledges financial support from WB-DST, India (ST/P/S&T/15G-20/2018), and CSIR, New Delhi (Sanction letter no. 01(3088)/21/EMR-II).

References

1 J. Li and D. J. Mooney, *Nat. Rev. Mater.*, 2016, **1**, 16071.
2 Y. Deng, M. Huang, D. Sun, Y. Hou, Y. Li, T. Dong, X. Wang, L. Zhang and W. Yang, *ACS Appl. Mater. Interfaces*, 2018, **10**, 37544–37554.
3 K.-H. Jeong, D. Park and Y.-C. Lee, *J. Polym. Res.*, 2017, **24**, 112.
4 M. Li, Y. Xiong and G. Qing, *Trends Anal. Chem.*, 2020, **124**, 115585.
5 Z. Wu, P. Zhang, H. Zhang, X. Li, Y. He, P. Qin and C. Yang, *J. Hazard. Mater.*, 2022, **421**, 126754.
6 M. A. Haque, T. Kurokawa and J. P. Gong, *Soft Matter*, 2012, **8**, 8008–8016.
7 K. J. Walker and S. V. Madihally, *J. Biomed. Mater. Res., Part B*, 2015, **103**, 1149–1160.
8 S. G. Rudisill, M. D. DiVito, A. Hubel and A. Stein, *Acta Biomater.*, 2015, **12**, 122–128.
9 M. Yamada, S. Sugaya, Y. Naganuma and M. Seki, *Soft Matter*, 2012, **8**, 3122–3130.
10 Y. Li, G. Huang, X. Zhang, L. Wang, Y. Du, T. J. Lu and F. Xu, *Biotechnol. Adv.*, 2014, **32**, 347–365.
11 S. Camarero-Espinosa, B. Rothen-Rutishauser, C. Weder and E. J. Foster, *Biomaterials*, 2016, **74**, 42–52.
12 S. Jana, S. K. L. Levengood and M. Zhang, *Adv. Mater.*, 2016, **28**, 10588–10612.
13 B. Sun, X.-J. Jiang, S. Zhang, J.-C. Zhang, Y.-F. Li, Q.-Z. You and Y.-Z. Long, *J. Mater. Chem. B*, 2015, **3**, 5389–5410.
14 G. C. Engelmayr Jr, M. Cheng, C. J. Bettinger, J. T. Borenstein, R. Langer and L. E. Freed, *Nat. Mater.*, 2008, **7**, 1003–1010.
15 M. Barrow, A. Eltmimi, A. Ahmed, P. Myers and H. Zhang, *J. Mater. Chem.*, 2012, **22**, 11615–11620.

16 K. Sano, Y. Ishida and T. Aida, *Angew. Chem., Int. Ed.*, 2018, **57**, 2532–2543.
17 S. Chatelin, M. Bernal, T. Deffieux, C. Papadacci, P. Flaud, A. Nahas, C. Boccara, J.-L. Gennisson, M. Tanter and M. Pernot, *Phys. Med. Biol.*, 2014, **59**, 6923–6940.
18 A. Osorio-Madrazo, M. Eder, M. Rueggeberg, J. K. Pandey, M. J. Harrington, Y. Nishiyama, J.-L. Putaux, C. Rochas and I. Burgert, *Biomacromolecules*, 2012, **13**, 850–856.
19 M. Liu, Y. Ishida, Y. Ebina, T. Sasaki, T. Hikima, M. Takata and T. Aida, *Nature*, 2015, **517**, 68–72.
20 X. Pei, T. Zan, H. Li, Y. Chen, L. Shi and Z. Zhang, *ACS Macro Lett.*, 2015, **4**, 1215–1219.
21 M. Chau, K. J. D. France, B. Kopera, V. R. Machado, S. Rosenfeldt, L. Reyes, K. J. W. Chan, S. Förster, E. D. Cranston, T. Hoare and E. Kumacheva, *Chem. Mater.*, 2016, **28**, 3406–3415.
22 A. J. Brown, *J. Chem. Soc.*, 1886, **51**, 638–643.
23 S.-P. Lin, I. L. Calvar, J. M. Catchmark, J.-R. Liu, A. Demirci and K.-C. Cheng, *Cellulose*, 2013, **20**, 2191–2219.
24 Y. Huang, C. Zhu, J. Yang, Y. Nie, C. Chen and D. Sun, *Cellulose*, 2014, **21**, 1–30.
25 W. Hu, S. Chen, J. Yang, Z. Li and H. Wang, *Carbohydr. Polym.*, 2014, **101**, 1043–1060.
26 A. Dobashi, J. Maruyama, Y. Shen, M. Nandi and H. Uyama, *Carbohydr. Polym.*, 2018, **200**, 381–390.
27 Y. Hu and J. M. Catchmark, *Biomacromolecules*, 2010, **11**, 1727–1734.
28 J. Hua, C. Liu, P. F. Ng and B. Fei, *Carbohydr. Polym.*, 2021, **259**, 117737.
29 K. Yu, S. Balasubramanian, H. Pahlavani, M. J. Mirzaali, A. A. Zadpoor and M.-E. Aubin-Tam, *ACS Appl. Mater. Interfaces*, 2020, **12**, 50748–50755.
30 J. Ran, P. Jiang, S. Liu, G. Sun, P. Yan, X. Shen and H. Tong, *Mater. Sci. Eng., C*, 2017, **78**, 130–140.
31 K. Okada, M. Nandi, J. Maruyama, T. Oka, T. Tsujimoto, K. Kondoh and H. Uyama, *Chem. Commun.*, 2011, **47**, 7422–7424.
32 H. Lin, J. Ou, Z. Zhang, J. Dong and H. Zou, *Chem. Commun.*, 2013, **49**, 231–233.
33 K. J. Barlow, X. Hao, T. C. Hughes, O. E. Hutt, A. Polyzos, K. A. Turner and G. Moad, *Polym. Chem.*, 2014, **5**, 722–732.
34 A. Magistris, P. Mustarelli, F. Parazzolia, E. Quartarone, P. Piaggio and A. Bottino, *J. Power Sources*, 2001, **97–98**, 657–660.
35 S. Yoneda, W. Han, U. Hasegawa and H. Uyama, *Polymer*, 2014, **55**, 3212–3216.
36 H. Uyama, *Koubunshi Ronbunshu*, 2010, **67**, 489–496.
37 M. Nandi, K. Okada and H. Uyama, *Funct. Mater. Lett.*, 2011, **4**, 407–410.
38 T. Kanno and H. Uyama, *RSC Adv.*, 2017, **7**, 33726–33732.
39 Y. Xin, T. Fujimoto and H. Uyama, *Polymer*, 2012, **53**, 2847–2853.
40 G. Wang and H. Uyama, *Colloid Polym. Sci.*, 2015, **293**, 2429–2435.
41 M. Takahashi, K. Tashiro and S. Amiya, *Macromolecules*, 1999, **32**, 5860–5871.
42 S. Yamanaka, K. Watanabe, N. Kitamura, M. Iguchi, S. Mitsuhashi, Y. Nishi and M. Uryu, *J. Mater. Sci.*, 1989, **24**, 3141–3145.
43 H. Qin, Y. Chen, J. Huang and Q. Wei, *Macromol. Mater. Eng.*, 2021, **306**, 2100159.
44 M. Martínez-Sanz, R. T. Olsson, A. Lopez-Rubio and J. M. Lagaron, *J. Appl. Polym. Sci.*, 2012, **124**, 1398–1408.
45 X. Chen, C. Chen, H. Zhang, Y. Huang, J. Yang and D. Sun, *Carbohydr. Polym.*, 2017, **173**, 547–555.
46 M. D. Donohue and G. L. Aranovich, *Adv. Colloid Interface Sci.*, 1998, **76-77**, 137–152.
47 H. Shim, A. Dobashi and H. Uyama, *Chem. Lett.*, 2016, **45**, 51–53.
48 M. Martínez-Sanz, R. T. Olsson, A. Lopez-Rubio and J. M. Lagaron, *Cellulose*, 2011, **18**, 335–347.
49 C. Qian, T. Higashigaki, T.-A. Asoh and H. Uyama, *ACS Appl. Mater. Interfaces*, 2020, **12**, 27518–27525.